Spin and parity assignments for low-lying states in the odd-mass nucleus ^{181}Ta

T. Shizuma [1], M. Omer [2,*], R. Hajima [1], and M. Koizumi [2]

[1] *Kansai Institute for Photon Science, National Institutes for Quantum Science and Technology, Kizugawa, Kyoto 619-0215, Japan*

[2] *Integrated Support Center for Nuclear Nonproliferation and Nuclear Security, Japan Atomic Energy Agency, Tokai, Ibaraki 319-1195, Japan*

(Received 7 February 2024; accepted 3 May 2024; published 20 May 2024)

Low-lying levels in the odd-mass nucleus ^{181}Ta have been populated via nuclear resonance fluorescence using a quasimonoenergetic, linearly polarized photon beam at the High Intensity γ-ray Source (HIγS) facility at Duke University. The spin and parity of the levels were determined from the azimuthal intensity asymmetry of resonantly scattered γ rays with respect to the polarization plane of the incident photon beam. The electric and magnetic dipole strengths were obtained for excitation energies from 2.2 to 3.2 MeV. The results are discussed in terms of the nuclear scissors mode.

DOI: 10.1103/PhysRevC.109.054320

I. INTRODUCTION

The scissors mode is a collective, orbital magnetic dipole ($M1$) excitation of deformed nuclei in which protons and neutrons oscillate against each other in a scissors-like fashion [1]. It is identified in well-deformed even-even nuclei by a relatively strong $M1$ excitation from the ground state to excited states with spin and parity of $J^\pi = 1^+$ and intrinsic-projection quantum number of $K = 1$. Since the discovery of the scissors mode in high-resolution inelastic electron scattering experiments [2], a large number of experimental data have been collected for rare-earth nuclei using nuclear resonance fluorescence (NRF) experiments [3,4], the Oslo method [5], and radiative neutron capture [6,7].

The systematics of the scissors mode in even-even nuclei is understood by using quadrupole deformation parameters [8,9] and has been extended to γ-soft nuclei [10,11]. The proportionality of the scissors mode strength to the square of the deformation parameter is understood by analysis based on a phenomenological sum-rule approach [12–14]. Theoretically, the existence of the scissors mode, an isovector $M1$ collective vibrational mode in deformed nuclei, has been predicted in the context of the two-rotor model [15] and the proton-neutron interacting boson model (IBM) [16].

Investigations of odd-mass nuclei have extended the systematics of the scissors mode. Since the first observation in ^{163}Dy [17] a variety of $M1$ strength distributions in nuclei around the rare-earth region have been obtained for ^{151,153}Eu [18], ^{155,157}Gd [19,20], ^{159}Tb [19], ^{161}Dy[20], ^{165}Ho [18,21,22], ^{167}Er [23], ^{169}Tm [21,22], ^{175}Lu [24], and ^{181}Ta [25,26] by the NRF technique and for ^{149}Sm [27], ^{167}Er [28], ^{171}Yb [29], and ^{181}Ta [30] by the Oslo method.

The interpretation of dipole transitions observed in NRF experiments requires information on their polarity [either $M1$ or electric dipole ($E1$)]. In recent decades it has been shown that a quasimonochromatic, linearly polarized photon beam produced by laser Compton scattering (LCS) considerably increases the experimental sensitivity, particularly to the parity quantum number of resonantly excited levels in even-even nuclei [31,32]. For odd-mass nuclei with nonzero ground-state spin, the modulation of the angular correlation function of NRF γ rays, which is essential for the measurement of parities using polarized photon beams, is much less pronounced than in even-even nuclei. Even in such a case, it was also demonstrated that spins and parities of excited states in odd-mass ^{87}Rb [33] and ^{207}Pb [34,35] could be determined with the help of polarized LCS photon beams. In the present study we apply a similar technique to odd-mass ^{181}Ta.

Previously, low-lying dipole strength distribution in ^{181}Ta was measured in an NRF experiment using bremsstrahlung [25]. While 37 levels are observed in the energy range between 1.8 and 3.4 MeV, their spins and parities remain to be unrevealed. In this paper, we report the results of an NRF measurement on ^{181}Ta using a quasimonochromatic, linearly polarized LCS photon beam.

II. EXPERIMENTAL PROCEDURE

The present NRF measurement was performed at the High Intensity γ-ray Source (HIγS) facility at the Free-Electron Laser Laboratory, Duke University in Durham, NC, USA [36]. Levels in ^{181}Ta were excited via NRF using a high-flux ($\approx 7 \times 10^7$ γ/s) quasimonoenergetic, linearly polarized photon beam. The polarization plane formed by the propagation direction of the electric vector was fixed horizontally. The beam irradiated a natural Ta target with a thickness of 4 mm and a diameter of 25.4 mm, placed inside an evacuated plastic tube to reduce the background counts due to scattering of the incident photons by air. An ^{27}Al target (25 mm thickness with a diameter of 32 mm) was also used for strength normalization of NRF γ rays of ^{181}Ta. The centroid energies of the incident photon beam were adjusted to 2.30, 2.45, 2.70, 2.85, and 3.05 MeV for the ^{181}Ta measurement and 3.00 MeV for the ^{27}Al measurement. The NRF γ rays were detected with four

*Permanent address: Physics Department, Faculty of Science, Assiut University, Assiut 71516, Egypt.

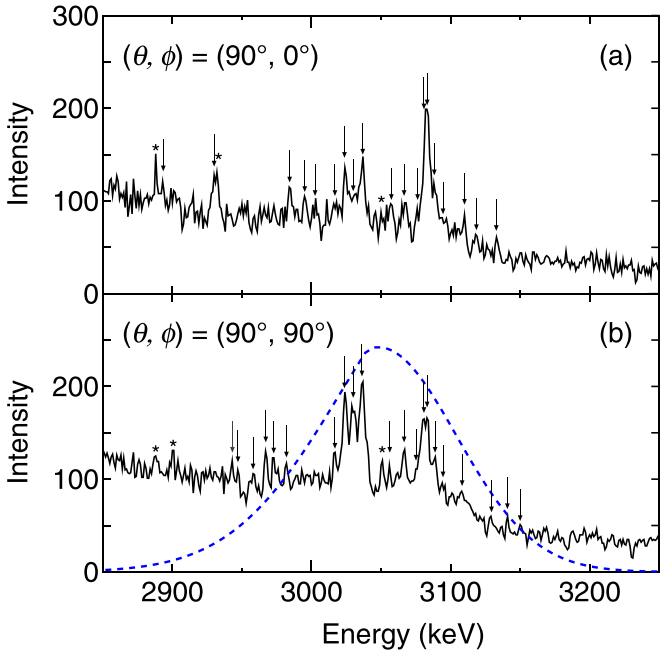

FIG. 1. Typical γ-ray spectra generated by a photon beam striking a ^{181}Ta target with a centroid energy of 3.05 MeV. The top (bottom) spectrum indicates photon scattering in parallel (perpendicular) to the polarization plane of the incident beam. The ground-state transitions and branching transitions, if observed, are shown with arrows and asterisks, respectively. The beam profile is overlaid (not to scale) as a dashed line in the lower panel.

high-purity germanium (HPGe) detectors with 55% and 60% detection efficiencies relative to the NaI scintillator detector (3 in. × 3 in.). These HPGe detectors were positioned at a scattering angle $\theta = 90^\circ$ relative to the beam with azimuthal angles of $\phi = 0^\circ$, 90° 180°, and 270° relative to the polarization plane of the incident photon beam, such that two of the detectors were placed horizontally and the other two vertically. Note that $\phi = 0^\circ$ (90°) is equivalent to $\phi = 180^\circ$ (270°) for the present detector geometry. The distance from the center of the target to the detectors was 15 cm. Lead and copper absorbers with thicknesses of 6 and 3 mm, respectively, were placed in front of the HPGe detectors to reduce the intensity of low energy photons hitting the detector. The energy and efficiency calibrations of the Ge detectors were carried out using a ^{56}Co standard source.

The photon beam was collimated by a lead collimator with a length of 20 cm and a cylindrical hole with a diameter of 2.2 cm. The energy distribution of the incident photon beam was measured with an HPGe detector placed in the beam periodically during the experiment. The beam flux was reduced during these measurements by inserting Cu attenuators into the beam further upstream. The relative efficiency of this HPGe detector was 123%. This HPGe detector was also used to monitor the beam flux by measuring the Compton scattering at about 13° off of a 1-mm-thick Cu plate. Typical photon scattering spectra of γ rays observed at $(\theta, \pi) = (90^\circ, 0^\circ)$ and $(90^\circ, 90^\circ)$ using the photon beam with a centroid energy of 3.050 MeV are shown in Figs. 1(a) and 1(b). An energy distribution of the photon beam corrected for detector response is also presented in Fig. 1(b). The energy width was approximately 4% in average. The details of the method are described in Ref. [37].

III. RESULTS

In photon scattering measurements, the energy-integrated scattering cross section I_s of a state at the excitation energy E_x can be deduced from the measured intensities of the respective transitions to the ground state [3]. In the present study, it was determined with respect to the known integrated scattering cross section I_s' of the state at 2982 keV in ^{27}Al (superscript $'$ denotes the case for the 2982-keV transition):

$$I_s = I_s' \frac{I_\gamma}{I_\gamma'} \frac{W' \Phi' N_t' \lambda_{tt}'}{W \Phi N_t \lambda_{tt}}. \tag{1}$$

Here, I_γ and I_γ' denote the efficiency-corrected intensities of a ground-state transition in ^{181}Ta and of the 2982-keV transition in ^{27}Al, respectively, obtained using summed spectra of γ rays emitted in parallel and perpendicularly to the polarization plane. W and W' are the angular distribution functions for these transitions at $\theta = 90^\circ$ for an unpolarized photon beam. Φ and Φ' are the photon fluxes at the energy of the considered level in ^{181}Ta and at 2982 keV for ^{27}Al. N_t and N_t' represent the numbers of ^{181}Ta and ^{27}Al target nuclei per unit area. The quantities λ_{tt} and λ_{tt}' are the correction factors of the atomic and nuclear self-absorption for the levels in ^{181}Ta and ^{27}Al. We used the integrated cross section of $I_s' = 31.9(7)$ eV b for the 2982-keV transition in ^{27}Al [38]. The determination of the integrated cross section relative to that of 2982-keV transition has an advantage that the efficiencies of the detectors and the photon flux are needed in relative units only.

The correction factor λ_{tt} can be numerically calculated by accounting for resonance width and thermal broadening through the following equations [39]:

$$\lambda_{tt} = \frac{\int \lambda \sigma_{\rm sc} dE}{\int \sigma_{\rm sc} dE}, \tag{2}$$

$$\lambda = \frac{1 - \exp\{-[\sigma_{\rm abs} + \sigma_e(1 + 1/\cos\theta)]N_t\}}{[\sigma_{\rm abs} + \sigma_e(1 + 1/\cos\theta)]N_t}, \tag{3}$$

where $\sigma_{\rm sc}$ and $\sigma_{\rm abs}$ are the thermally broadened resonance cross sections for scattering and absorption (see Ref. [39] for details) and σ_e is the atomic scattering cross section [40]. Equation (3) represents the thick target correction for the resonance shape and must be integrated over the energy E to obtain the scalar value λ_{tt} as shown in Eq. (2).

The integrated scattering cross section I_s is related to the total decay width Γ and the partial decay width Γ_0 to the ground state according to

$$I_s = \left(\frac{\pi \hbar c}{E_x}\right)^2 \frac{g \Gamma_0^2}{\Gamma}, \tag{4}$$

where g is a spin factor defined as $(2J_x + 1)/(2J_0 + 1)$ with J_0 and J_x being the spins of the ground state and the excited state.

In the present study, spins and parities J^π of resonantly excited states are determined based on azimuthal asymmetry

of angular distribution function of scattering γ rays. The angular distribution function of a γ_2 ray deexciting a level with angular momentum J_1 to a level J_2 via a mixed transition of type (L_2, L_2'), where $L_2' = L_2 + 1$, relative to an absorbed polarized γ_1 ray exciting the level J_1 from a level J_0 via a mixed transition of type (L_1, L_1'), where $L_1' = L_1 + 1$, is given by

$$W(\theta,\phi) = \sum_{\nu=0}^{\text{even}} B_\nu(\vec{\gamma}_1)A_\nu(\gamma_2)P_\nu(\cos\theta) + (\pm)_{L_1}\cos(2\phi) \times \sum_{\nu=2}^{\text{even}} B'_\nu(\vec{\gamma}_1)A_\nu(\gamma_2)P^{(2)}_\nu(\cos\theta), \quad (5)$$

where $P_\nu(\cos\theta)$ and $P^{(2)}_\nu(\cos\theta)$ are Legendre polynomials and unnormalized associated Legendre polynomials, respectively [3,4,41,42]. The first term of the right-hand side of the equation is the angular distribution function for an unpolarized γ_1 ray. The factors $(\pm)_{L_1}$ are $+1$ (-1) if L_1 is of electric (magnetic) character. The expansion coefficients A_ν, B_ν, and B'_ν are given by the phase convention of Krane, Steffen, and Wheeler in Ref. [43]. Equation (5) includes multipole mixing ratios δ_1 and δ_2 for the γ_1- and γ_2-ray transitions, respectively. For the case of elastic scattering, the levels J_0 and J_2 are identical to each other so that $L_1 = L_2$ and $|\delta_1| = |\delta_2|$.

Considering dipole excitation of the ground state of ^{181}Ta with $J^\pi_0 = 7/2^+$, spins and parities of resonantly excited states could only be $J^\pi = 5/2^\pm$, $7/2^\pm$, or $9/2^\pm$. The angular distribution function for dipole radiation with $\delta = 0$, which may be a reasonable assumption for dipole transitions observed in NRF measurements, can be reduced to

$$W(\theta,\phi) = W(\theta) \pm C_1(1 - \cos^2\theta)\cos2\phi, \quad (6)$$

where $W(\theta)(= C_1\cos^2\theta + C_2)$ is the angular correlation function for an unpolarized photon beam. C_1 and C_2 are coefficients determined by A_ν, B_ν, and B'_ν. Here, the plus (minus) sign corresponds to $M1$ ($E1$) transitions.

Using the azimuthal angular distributions at $(\theta,\phi) = (90^\circ, 0^\circ)$ and $(90^\circ, 90^\circ)$, the azimuthal intensity asymmetry Σ is defined in Ref. [31] as

$$\Sigma = \frac{W(90^\circ, 0^\circ) - W(90^\circ, 90^\circ)}{W(90^\circ, 0^\circ) + W(90^\circ, 90^\circ)}. \quad (7)$$

$W(90^\circ, 0^\circ)$ and $W(90^\circ, 90^\circ)$ are obtained as $C_2 \pm C_1$ and $C_2 \mp C_1$, respectively, from Eq. (6). Substituting these azimuthal angular distributions into Eq. (7), Σ becomes $\pm C_1/C_2$. The expected values of C_1, C_2, and Σ for $7/2^+ \to 5/2^\pm$, $7/2^\pm$, or $9/2^\pm \to 7/2^+$ photon scattering cascades are summarized in Table I.

The corresponding intensity asymmetry A of the observed NRF γ rays is given by

$$A = \frac{N_\parallel - N_\perp}{N_\parallel + N_\perp} = q\Sigma, \quad (8)$$

where $N_\parallel$ ($N_\perp$) represents the measured intensity of NRF γ rays detected at $\theta = 90^\circ$ in a plane parallel (perpendicular) to the polarization plane of incident photons. Here, q is the experimental sensitivity, which is less than unity because of the finite solid angle of the HPGe detectors and the spatially extended target. In the present case, q is estimated to be approximately 0.98 by the numerical simulation assuming that the degree of polarization of the incident photon beam is nearly 100%.

TABLE I. C_1 and C_2 values and azimuthal intensity asymmetries Σ deduced for the $7/2^+ \to 5/2^\pm$, $7/2^\pm$, or $9/2^\pm \to 7/2^+$ photon scattering cascades with the assumption of $\delta_1 = \delta_2 = 0$ for angular distribution function.

J^π of resonant states[a]	C_1	C_2	Σ[a]
$5/2^\pm$	$\frac{3}{112}$	$\frac{111}{112}$	±0.027
$7/2^\pm$	$\frac{6}{21}$	$\frac{19}{21}$	±0.32
$9/2^\pm$	$\frac{33}{240}$	$\frac{229}{240}$	±0.14

[a]$\pm$ signs in the first and fourth columns correspond to each other in the same order.

The present experimental results are summarized in Table II. We observed 46 resonant states at excitation energies between 2.2 and 3.2 MeV. Spins and parities for these states were assigned by comparison of the measured and calculated azimuthal intensity asymmetries by taking a confidence interval of $\pm1\sigma$ in Fig. 2. A comparison of the $g\Gamma_0$ values obtained in the present experiment with those from previous work [25] is also shown in Table II and Fig. 3. At lower excitation energies the present results are in good agreement with those previously reported. However, the strength of the 3080-keV transition is about 20% of the value from the previous work. This would be in part due to doublet nature of the 3080-keV transition with the 3083-keV transition. The summed strength of these transitions amounts to about 70% of the previous value. The present $g\Gamma_0$ values are systematically smaller for higher excitation energies. Considering the higher bremsstrahlung endpoint energy of 4.1 MeV used in the previous measurement [25], this is likely due to the results of feeding from higher-lying levels. Similar effects are observed

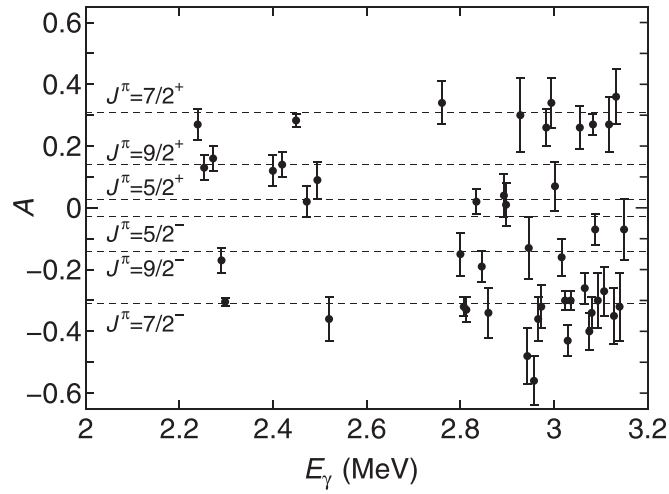

FIG. 2. Azimuthal intensity asymmetry A obtained for the transitions of ^{181}Ta. The horizontal dashed lines indicate the calculated asymmetry for transitions from $J^\pi = 5/2^\pm$, $7/2^\pm$, or $9/2^\pm$ resonant states, obtained with the assumption of $\delta_1 = \delta_2 = 0$ for the angular distribution function.

TABLE II. Excitation energies E_x, azimuthal intensity asymmetry A, spins and parities J^π, $g\Gamma_0$ values, branching ratios to the ground state Γ_0/Γ, and reduced transition probabilities $B(E1)\uparrow$ and $B(M1)\uparrow$ obtained in the present work. $g\Gamma_0$ values reported in previous work are listed for comparison.

E_x (keV)	A	J^π [a]	$g\Gamma_0$ [b] (meV)	Γ_0/Γ	$B(E1)\uparrow$ ($\times10^{-3}$ e^2fm^2)	$B(M1)\uparrow$ ($\times10^{-3}$ μ_N^2)	$g\Gamma_0$ [c] (meV)
2239.1(2)	0.27(5)	$7/2^+$	3.23(27)	1.0		24.9(21)	2.81(64)
2252.9(3)	0.13(4)	$9/2^+$	4.9(4)	1.0		37.2(27)	3.81(71)
2272.0(2)	0.16(4)	$9/2^+$	3.36(24)	1.0		24.8(18)	4.86(79)
2289.9(3)	−0.17(4)	$9/2^-$	2.32(17)	1.0	0.185(14)		4.43(75)
2297.6(1)	−0.30(1)	$7/2^-$	36.3(23)	0.84(1)	2.86(18)		39.00(391)
2399.6(5)	0.12(5)	$9/2^+$	9.3(8)	0.38(2)		58(5)	7.65(118)
2419.4(3)	0.14(4)	$9/2^+$	4.9(4)	0.68(2)		30.0(23)	5.28(96)
2449.2(2)	0.28(2)	$(7/2^+)$	11.8(8)	0.76(1)		69(5)	11.95(153)
2472.0(4)	0.02(5)	5/2	1.97(15)	1.0	0.124(10)	11.3(9)	
2494.7(3)	0.09(6)	$9/2^+$	2.17(18)	1.0		12.1(10)	
2519.6(3)	−0.36(7)	$7/2^-$	2.18(22)	1.0	0.130(13)		3.96(71)
2760.7(3)	0.34(7)	$7/2^+$	4.4(4)	1.0		18.0(18)	3.25(70)
2800(1)	−0.15(7)	$9/2^-$	2.40(23)	1.0	0.104(10)		2.18(64)
2807.3(3)	−0.32(3)	$7/2^-$	11.9(9)	0.77(1)	0.52(4)		7.71(108)
2812.7(3)	−0.33(4)	$7/2^-$	7.3(5)	1.0	0.312(23)		6.32(95)
2834.2(4)	0.02(4)	$5/2^+$	3.84(29)	1.0		14.6(11)	5.21(87)
2845.6(4)	−0.19(5)	$9/2^-$	2.77(22)	1.0	0.115(9)		3.31(73)
2859.9(9)	−0.34(8)	$7/2^-$	1.17(12)	1.0	0.048(5)		
2893.0(5)	0.04(7)	5/2	1.85(18)	1.0	0.073(7)	6.6(6)	3.66(77)
2897.5(4)	0.01(7)	5/2	2.23(21)	1.0	0.088(8)	7.9(7)	6.86(100)
2928.0(4)	0.30(12)	$7/2^+$	1.48(21)	1.0		5.1(7)	3.35(75)
2942.9(5)	−0.48(9)	$(7/2^-)$	4.2(5)	1.0	0.157(19)		
2946.0(9)	−0.13(10)	$9/2^-$	4.45(53)	1.0	0.166(20)		
2957.2(7)	−0.56(8)	$(7/2^-)$	4.52(51)	1.0	0.167(19)		
2966.1(3)	−0.36(7)	$7/2^-$	5.5(5)	1.0	0.200(20)		6.92(96)
2972.7(6)	−0.32(7)	$7/2^-$	5.1(5)	1.0	0.185(18)		
2983.4(4)	0.26(6)	$7/2^+$	5.7(5)	1.0		18.7(16)	
2994.3(4)	0.34(8)	$7/2^+$	2.56(27)	1.0		8.2(9)	
3002(1)	0.07(8)	$5/2^+$,$9/2^+$	2.27(23)	1.0		7.3(7)	
3016.2(6)	−0.16(6)	$9/2^-$	3.00(27)	1.0	0.105(9)		3.17(73)
3023.5(2)	−0.30(3)	$7/2^-$	10.2(8)	0.79(1)	0.352(26)		11.06(134)
3029.2(2)	−0.43(5)	$(7/2^-)$	6.6(5)	1.0	0.225(17)		9.7(123)
3035.4(2)	−0.30(3)	$7/2^-$	9.9(7)	0.88(1)	0.339(25)		13.79(155)
3055.1(5)	0.26(7)	$7/2^+$	4.0(4)	0.53(3)		12.1(13)	6.55(113)
3065.6(5)	−0.26(5)	$7/2^-$	7.1(6)	0.56(2)	0.234(19)		7.04(110)
3075.3(9)	−0.40(6)	$(7/2^-)$	3.2(3)	0.81(2)	0.104(10)		8.49(137)
3080.3(5)	−0.34(5)	$7/2^-$	4.8(4)	1.0	0.158(13)		22.21(235)
3083.1(4)	0.27(3)	$(7/2^+)$	10.9(8)	1.0		32.1(23)	
3087.8(4)	−0.07(5)	$5/2^-$	4.8(4)	1.0	0.154(12)		5.87(94)
3093.5(8)	−0.30(9)	$7/2^-$	1.79(20)	1.0	0.058(6)		3.63(78)
3107.0(8)	−0.27(8)	$7/2^-$	4.0(5)	0.68(3)	0.127(14)		12.17(155)
3117.5(6)	0.27(9)	$7/2^+$	2.8(3)	1.0		8.0(9)	
3127.9(5)	−0.35(9)	$7/2^-$	2.9(4)	1.0	0.091(11)		
3132.4(4)	0.36(9)	$7/2^+$	3.8(4)	1.0		10.6(12)	
3139.9(4)	−0.32(11)	$7/2^-$	2.9(4)	1.0	0.089(12)		
3149.5(6)	−0.07(10)	5/2, $9/2^-$	5.4(6)	1.0	0.164(19)	14.9(17)	

[a]The assignments are based on comparison of the measured and calculated azimuthal intensity asymmetries by taking a confidence interval of $\pm1\sigma$. When the data points did not overlap with the expectations within the $\pm1\sigma$ limit, we assigned the spin and parity for which the expectation value is closest to the data and listed them with parentheses (see Fig. 2).
[b]This work.
[c]Taken from Ref. [25].

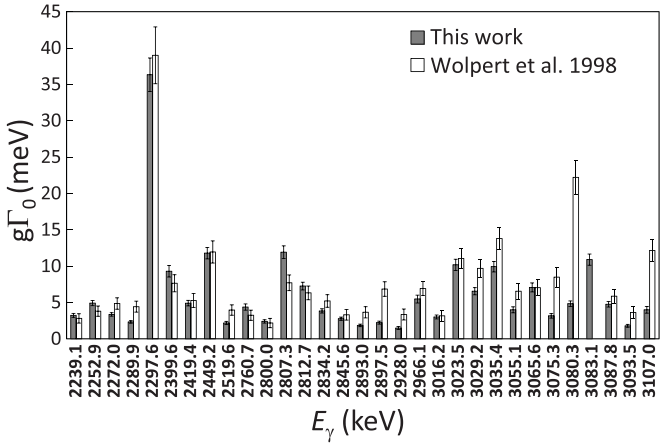

FIG. 3. Comparison of the $g\Gamma_0$ values obtained in the present experiment (gray bars) with those from Wolpert *et al.* [25] (white bars). The 3080- and 3083-keV transitions are possibly a doublet (see text for details).

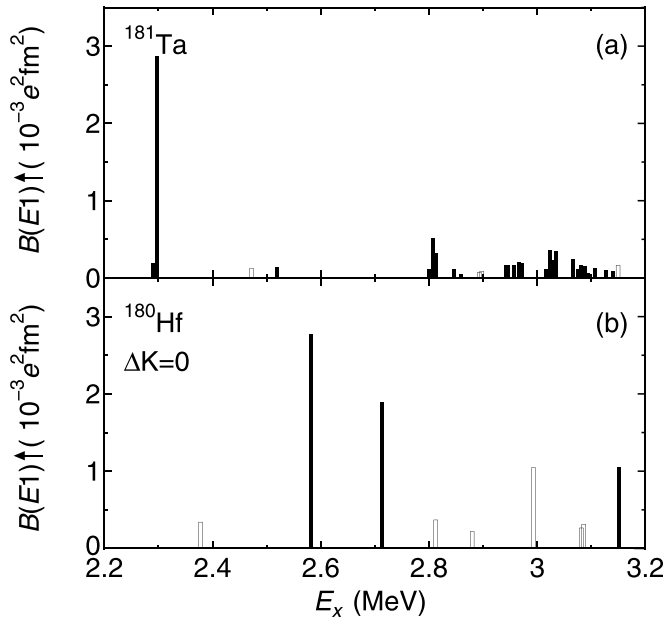

FIG. 4. $B(E1)\uparrow$ values deduced from the present NRF experiment are shown in the upper panel (a). If the parity of the resonant state is known (unknown) from the azimuthal intensity asymmetry measurement, the data are plotted with solid (open) bars. In the lower panel (b), $B(E1)\uparrow$ values for $\Delta K = 0$ (unknown ΔK) transitions found in ^{180}Hf [45] are plotted with solid (open) bars. Spin-1 states with $K = 0$ in even-even nuclei have most probably a negative parity (see text).

in ^{90}Zr, where levels in the range of $E_x \approx 4$ to 6 MeV are mainly fed by levels above $E_x \approx 6$ MeV [44].

Three transitions were observed above 3.3 MeV in the previous experiment [25]. However, in the energy range between 3.4 and 4.0 MeV no dipole transition is reported. This is in contrast to the results for ^{180}Hf, showing 21 levels observed in the same energy range [45]. The reason for this difference probably is an increased strength fragmentation leading to smaller strengths of the individual transitions in odd-mass nuclei.

IV. DISCUSSION

The largest strength is carried by a ground-state transition from the 2298-keV state with $g\Gamma_0 = 36.3(23)$ meV as shown in Fig. 3, corresponding to $I_s = 22.2(14)$ eV b. It takes about 23% of the total dipole transition strength observed in the present NRF measurement. Other transitions are relatively weak, less than $\approx 1/4$, compared to this transition.

The reduced transition probabilities $B(E1)\uparrow$ and $B(M1)\uparrow$ can be extracted from $g\Gamma_0$ using the following relationships:

$$B(E1)\uparrow = 0.955\frac{g\Gamma_0}{E_\gamma^3} \times 10^{-3}\ e^2\mathrm{fm}^2, \tag{9}$$

$$B(M1)\uparrow = 0.0866\frac{g\Gamma_0}{E_\gamma^3}\ \mu_N^2, \tag{10}$$

where Γ_0 and E_γ are given in units of meV and MeV, respectively. The deduced $E1$ and $M1$ excitation probabilities are summarized in Table II. From the present work, the total $E1$ and $M1$ strengths at excitation energies from 2.2 to 3.2 MeV were obtained as $\Sigma B(E1)\uparrow_{2.2\text{–}3.2\mathrm{MeV}} = 7.63(20) \times 10^{-3}\ e^2\mathrm{fm}^2$ and $\Sigma B(M1)\uparrow_{2.2\text{–}3.2\mathrm{MeV}} = 0.432(9)\,\mu_N^2$, respectively. Here, the strengths for the unknown parity states at 2472, 2893, 2897, and 3149 keV are included in both the total $E1$ and $M1$ strengths. Therefore, the above total strengths indicate upper limits obtained from the present measurement. The uncertainties of the total $E1$ and $M1$ strengths were calculated by adding those of each strength in quadrature.

Outside of the above energy range, seven transitions are reported without multipolarity assignments [25]. Assuming that all these transitions are $E1$ ($M1$), we added their strengths to the present total $E1$ ($M1$) strength. Then, we obtained $\Sigma B(E1)\uparrow_{1.8\text{–}3.41\mathrm{MeV}} = 10.21(27) \times 10^{-3}\ e^2\mathrm{fm}^2$ or $\Sigma B(M1)\uparrow_{1.8\text{–}3.41\mathrm{MeV}} = 0.664(19)\,\mu_N^2$ at the energy range from 1.8 to 3.41 MeV as upper limits. The strength attributed to the $M1$ excitation is about 40% of the total dipole strength obtained here, which is comparable to those known for the neighboring even-even W and Hf nuclei.

In Figs. 4 and 5, the $E1$ and $M1$ excitation probabilities are compared with the results from the previous study on the isotone ^{180}Hf [45]. Note that for ^{180}Hf the parity assignments are based on the Alaga rule [46] which predicts that negative-parity (positive-parity) states with $J = 1$ in axially symmetric even-even nuclei mostly decay with $\Delta K = 0$ (1) [45,47].

The 2298-keV transition having the largest dipole strength observed in the present NRF measurement is assigned $E1$ multipolarity. Its $E1$ strength equals to $B(E1)\uparrow = 2.86(18) \times 10^{-3}\ e^2\mathrm{fm}^2$, which can be compared to one that obtained for ^{180}Hf, $B(E1)\uparrow = 2.78(39) \times 10^{-3}\ e^2\mathrm{fm}^2$ at 2582 keV [45]. The other $E1$ strengths are fragmented into rather weak transitions with $B(E1)\uparrow \lesssim 0.5 \times 10^{-3}\ e^2\mathrm{fm}^2$ as shown in Fig. 4(a). This is contrast to the ^{180}Hf case where fewer transitions are responsible for the observed $E1$ strengths. The increased strength fragmentation in ^{181}Ta can be attributed to high level density expected for odd-mass deformed nuclei.

The $M1$ strength in ^{181}Ta is more fragmented and reduced as compared to ^{180}Hf, as shown in Fig. 5. Note that the scales

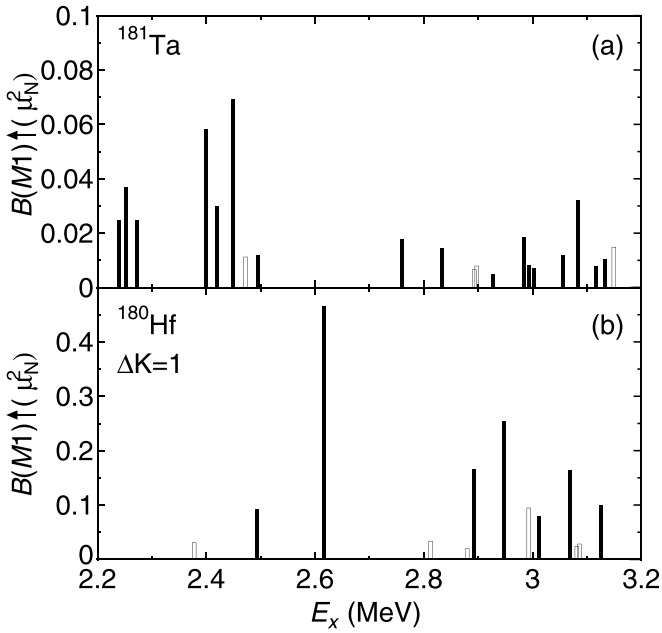

FIG. 5. $B(M1)\uparrow$ values deduced from the present NRF experiment are shown in the upper panel (a). If the parity of the resonant state is known (unknown) from the azimuthal intensity asymmetry measurement, the data are plotted with solid (open) bars. In the lower panel (b), $B(M1)\uparrow$ values for $\Delta K = 1$ (unknown ΔK) transitions found in ^{180}Hf [45] are plotted with solid (open) bars. Spin-1 states with $K = 1$ in even-even nuclei have most probably a positive parity (see text). Note that the scale in the upper panel is enlarged by a factor of 5.

of Figs. 5(a) and 5(b) differ by a factor of 5. The total $M1$ strength attributed to the scissors mode in ^{180}Hf amounts to $\Sigma B(M1)\uparrow_{2.4\text{–}3.7\text{MeV}} = 1.61(7)\,\mu_N^2$ [45]. This value is much higher than that observed in ^{181}Ta [$\Sigma B(M1)\uparrow_{2.2\text{–}3.2\text{MeV}} = 0.432(9)\,\mu_N^2$ or $\Sigma B(M1)\uparrow_{1.8\text{–}3.41\text{MeV}} = 0.664(19)\,\mu_N^2$]. This accords with the systematics that the scissors mode $M1$ strengths observed in odd-mass nuclei are a factor of 2 to 3 smaller than those in even-even neighbors [48]. It has been suggested that the missing strength could be shifted to higher energies and/or that it might be distributed over a large number of unresolved weak transitions that escape detection [48]. A statistical fluctuation analysis to identify this missing strength hidden in the background has been applied to several odd-mass nuclei [22,48], but is beyond the scope of the present paper.

The $M1$ strength distribution shown in Fig. 5(a) can be separated into two parts, i.e., 2.2–2.6 and 2.6–3.2 MeV with split centroids located at 2.4 and 3.0 MeV. This splitting can be interpreted by means of γ deformation which describes the deviation from axial symmetry or the nuclear triaxial deformation [49]. For the case of ^{181}Ta, a γ deformation of about 12° is deduced from the model based on the sum-rule approach [14,49], in agreement with the results from the Oslo method [50]. However, this model predicts that a higher-lying scissors mode component has the largest strength, which is inconsistent with the measurement, as confirmed in the actinide region [51]. Further experimental and theoretical investigations are desired to uncover the origin of the splitting of the scissor mode.

V. SUMMARY

We have performed a nuclear resonance fluorescence experiment on the odd-mass nucleus ^{181}Ta using a quasi-monoenergetic, linearly polarized photon beam generated by laser Compton scattering. A total of 46 resonant states were confirmed at excitation energies from 2.2 to 3.2 MeV. Their spin and parity quantum numbers were deduced based on the azimuthal intensity asymmetries of scattered γ rays with respect to the polarization plane of the incident photon beam. The total dipole strengths of $\Sigma B(E1)\uparrow_{2.2\text{–}3.2\text{MeV}} = 7.63(20) \times 10^{-3}\ e^2\text{fm}^2$ and $\Sigma B(M1)\uparrow_{2.2\text{–}3.2\text{MeV}} = 0.432(9)\,\mu_N^2$ were obtained. The measured $M1$ strength is consistent with the systematics concerning the fragmentation and reduction of the scissors mode strength in odd-mass deformed nuclei in the region. The energy splitting of the $M1$ strength may indicate nuclear triaxiality.

ACKNOWLEDGMENTS

We would like to acknowledge the support provided by the staff at the High Intensity γ-ray Source facility. This work was a part of the study of NRF phenomenon aiming at nuclear security and safeguards applications, being supported by the subsidiary for "promotion of strengthening nuclear security or the like" of the Ministry of Education, Culture, Sports, Science and Technology (MEXT), Japan. T.S. was supported by JSPS KAKENHI Grants No. 17K05482 and No. 20K04007.

[1] K. Heyde, P. von Neumann-Cosel, and A. Richter, Rev. Mod. Phys. **82**, 2365 (2010).
[2] D. Bohle, A. Richter, W. Steffen, A. E. L. Dieperink, N. Lo Iudice, F. Palumbo, and O. Scholten, Phys. Lett. B **137**, 27 (1984).
[3] U. Kneissl, H. H. Pitz, and A. Zilges, Prog. Part. Nucl. Phys. **37**, 349 (1996).
[4] A. Zilges, D. L. Balabanski, J. Isaak, and N. Pietrall, Prog. Part. Nucl. Phys. **122**, 103903 (2022).
[5] A. Schiller, L. Bergholt, M. Guttormsen, E. Melby, J. Rekstad, and S. Siem, Nucl. Instrum. Methods Phys. Res., Sect. A **447**, 498 (2000).
[6] M. Krtička, F. Bečvář, J. Honzátko, I. Tomandl, M. Heil, F. Käppeler, R. Reifarth, F. Voss, and K. Wisshak, Phys. Rev. Lett. **92**, 172501 (2004).
[7] B. Baramsai, EPJ Web Conf. **93**, 01037 (2015).
[8] P. von Neumann-Cosel, J. N. Ginocchio, H. Bauer, and A. Richter, Phys. Rev. Lett. **75**, 4178 (1995).

[9] N. Pietralla, P. von Brentano, R.-D. Herzberg, U. Kneissl, J. Margraf, H. Maser, H. H. Pitz, and A. Zilges, Phys. Rev. C **52**, R2317(R) (1995).

[10] P. von Brentano, J. Eberth, J. Enders, L. Esser, R.-D. Herzberg, N. Huxel, H. Meise, P. von Neumann-Cosel, N. Nicolay, N. Pietralla, H. Prade, J. Reif, A. Richter, C. Schlegel, R. Schwengner, S. Skoda, H. G. Thomas, I. Wiedenhöver, G. Winter, and A. Zilges, Phys. Rev. Lett. **76**, 2029 (1996).

[11] H. Maser, N. Pietralla, P. von Brentano, R.-D. Herzberg, U. Kneissl, J. Margraf, H. H. Pitz, and A. Zilges, Phys. Rev. C **54**, R2129 (1996).

[12] N. Lo Iudice and A. Richter, Phys. Lett. B **304**, 193 (1993).

[13] E. Lipparini and S. Stringari, Phys. Lett. B **130**, 139 (1983).

[14] E. Lipparini and S. Stringari, Phys. Rep. **175**, 103 (1989).

[15] N. L. Iudice and F. Palumbo, Phys. Rev. Lett. **41**, 1532 (1978).

[16] F. Iachello, Nucl. Phys. A **358**, 89 (1981).

[17] I. Bauske, J. M. Arias, P. von Brentano, A. Frank, H. Friedrichs, R. D. Heil, R.-D. Herzberg, F. Hoyler, P. Van Isacker, U. Kneissl, J. Margraf, H. H. Pitz, C. Wesselborg, and A. Zilges, Phys. Rev. Lett. **71**, 975 (1993).

[18] A. Nord, J. Enders, A. E. de Almeida Pinto, D. Belic, P. von Brentano, C. Fransen, U. Kneissl, C. Kohstall, A. Linnemann, P. von Neumann-Cosel, N. Pietralla, H. H. Pitz, A. Richter, F. Stedile, and V. Werner, Phys. Rev. C **67**, 034307 (2003).

[19] A. Nord, A. Schiller, T. Eckert, O. Beck, J. Besserer, P. von Brentano, R. Fischer, R.-D. Herzberg, D. Jäger, U. Kneissl, J. Margraf, H. Maser, N. Pietralla, H. H. Pitz, M. Rittner, and A. Zilges, Phys. Rev. C **54**, 2287 (1996).

[20] J. Margraf, T. Eckert, M. Rittner, I. Bauske, O. Beck, U. Kneissl, H. Maser, H. H. Pitz, A. Schiller, P. von Brentano, R. Fischer, R.-D. Herzberg, N. Pietralla, A. Zilges, and H. Friedrichs, Phys. Rev. C **52**, 2429 (1995).

[21] P. Von Neumann-Cosel, Prog. Part. Nucl. Phys. **38**, 213 (1997).

[22] N. Huxel, R. von Brentano, J. Eberth, J. Enders, R.-D. Herzberg, R. von Neumann-Cosel, N. Nicolay, N. Pietralla, H. Prade, C. Rangacharyulu, J. Reif, A. Richter, C. Schlegel, R. Schwengner, S. Skoda, H. G. Thomas, I. Wiedenhöver, G. Winter, and A. Zilges, Nucl. Phys. A **645**, 239 (1999).

[23] C. Schlegel, P. von Neumann-Cosel, A. Richter, and P. Van Isacker, Phys. Lett. B **375**, 21 (1996).

[24] R.-D. Herzberg, C. Fransen, R. Fischer, O. Beck, D. Belic, J. Besserer, P. von Brentano, Th. Eckert, U. Kneissl, B. Krischok, J. Margraf, H. Maser, A. Nord, N. Pietralla, H. H. Pitz, A. Wolpert, and A. Zilges, Phys. Rev. C **56**, 2484 (1997).

[25] A. Wolpert, O. Beck, D. Belic, J. Besserer, P. von Brentano, T. Eckert, C. Fransen, R.-D. Herzberg, U. Kneissl, J. Margraf, H. Maser, A. Nord, N. Pietralla, and H. H. Pitz, Phys. Rev. C **58**, 765 (1998).

[26] C. T. Angell, R. Hajima, T. Shizuma, B. Ludewigt, and B. J. Quiter, Phys. Rev. Lett. **117**, 142501 (2016).

[27] S. Siem, M. Guttormsen, K. Ingeberg, E. Melby, J. Rekstad, A. Schiller, and A. Voinov, Phys. Rev. C **65**, 044318 (2002).

[28] E. Melby, M. Guttormsen, J. Rekstad, A. Schiller, S. Siem, and A. Voinov, Phys. Rev. C **63**, 044309 (2001).

[29] U. Agvaanluvsan, A. Schiller, J. A. Becker, L. A. Bernstein, P. E. Garrett, M. Guttormsen, G. E. Mitchell, J. Rekstad, S. Siem, A. Voinov, and W. Younes, Phys. Rev. C **70**, 054611 (2004).

[30] C. P. Brits, M. Wiedeking, F. L. Bello Garrote, D. L. Bleuel, F. Giacoppo, A. Gorgen, M. Guttormsen, K. Hadynska-Klek, T. W. Hagen, V. W. Ingeberg, B. V. Kheswa, M. Klintefjord, A. C. Larsen, K. L. Malatji, H. T. Nyhus, P. Papka, T. Renstrøm, S. Rose, E. Sahin, S. Siem, G. M. Tveten, and F. Zeiser, EPJ Web Conf. **146**, 05012 (2017).

[31] N. Pietralla, Z. Berant, V. N. Litvinenko, S. Hartman, F. F. Mikhailov, I. V. Pinayev, G. Swift, M. W. Ahmed, J. H. Kelley, S. O. Nelson, R. Prior, K. Sabourov, A. P. Tonchev, and H. R. Weller, Phys. Rev. Lett. **88**, 012502 (2001).

[32] T. Shizuma, T. Hayakawa, H. Ohgaki, H. Toyokawa, T. Komatsubara, N. Kikuzawa, A. Tamii, and H. Nakada, Phys. Rev. C **78**, 061303(R) (2008).

[33] J. Wilhelmy, M. Müscher, G. Rusev, R. Schwengner, R. Beyer, M. Bhike, P. Erbacher, F. Fiedler, U. Friman-Gayer, J. Glorius, R. Greifenhagen, S. Hammer, T. Hensel, J. Isaak, A. R. Junghans, Krishichayan, B. Löher, S. E. Müller, N. Pietralla, S. Reinicke, D. Savran *et al.*, Phys. Rev. C **102**, 044327 (2020).

[34] N. Pietralla, T. C. Li, M. Fritzsche, M. W. Ahmed, T. Ahn, A. Costin, J. Enders, J. Li, S. Müller, P. von Neumann-Cosel, I. V. Pinayev, V. Yu. Ponomarev, D. Savran, A. P. Tonchev, W. Tornow, H. R. Weller, V. Werner, Y. K. Wu, and A. Zilges, Phys. Lett. B **681**, 134 (2009).

[35] T. Shizuma, F. Minato, M. Omer, T. Hayakawa, H. Ohgaki, and S. Miyamoto, Phys. Rev. C **103**, 024309 (2021).

[36] H. R. Weller, M. W. Ahmed, H. Gao, W. Tornow, Y. K. Wu, M. Gai, and R. Miskimen, Prog. Part. Nucl. Phys. **62**, 257 (2009).

[37] C. T. Angell, R. Hajima, T. Hayakawa, T. Shizuma, H. J. Karwowski, and J. Silano, Phys. Rev. C **90**, 054315 (2014).

[38] N. Pietralla, I. Bauske, O. Beck, P. von Brentano, W. Geiger, R.-D. Herzberg, U. Kneissl, J. Margraf, H. Maser, H. H. Pitz, and A. Zilges, Phys. Rev. C **51**, 1021 (1995).

[39] F. Metzger, in *Progress in Nuclear Physics*, edited by O. Frisch (Pergamon, New York, 1959), Vol. 7, pp. 53–88.

[40] M. J. Berger *et al.*, *XCOM: Photon Cross Sections Database* (National Institute of Standards and Technology, Gaithersburg, MD, 2010).

[41] N. Pietralla, M. W. Ahmed, C. Fransen, V. N. Litvinenko, A. P. Tonchev, and H. R. Weller, AIP Conf. Proc. **656**, 365 (2003).

[42] L. W. Fagg and S. S. Hanna, Rev. Mod. Phys. **31**, 711 (1959).

[43] K. S. Krane, R. M. Steffen, and R. M. Wheeler, At. Data Nucl. Data Tables **11**, 351 (1973).

[44] R. Schwengner, G. Rusev, N. Tsoneva, N. Benouaret, R. Beyer, M. Erhard, E. Grosse, A. R. Junghans, J. Klug, K. Kosev, H. Lenske, C. Nair, and K. D. Schilling, and A. Wagner, Phys. Rev. C **78**, 064314 (2008).

[45] N. Pietralla, O. Beck, J. Besserer, P. von Brentano, T. Eckert, R. Fischer, C. Fransen, R.-D. Herzberg, D. Jäger, R. V. Jolos, U. Kneissl, B. Krischok, J. Margraf, H. Maser, A. Nord, H. H. Pitz, M. Rittner, A. Schiller, and A. Zilges, Nucl. Phys. A **618**, 141 (1997).

[46] G. Alaga, K. Alder, A. Bohr, and B. R. Mottelson, Kgl. Danske Videnskab. Selskab Mat.-Fys. Medd. **29**, No. 9 (1955).

[47] D. Savran, S. Müller, A. Zilges, M. Babilon, M. W. Ahmed, J. H. Kelley, A. Tonchev, W. Tornow, H. R. Weller, N. Pietralla, J. Li, I. V. Pinayev, and Y. K. Wu, Phys. Rev. C **71**, 034304 (2005).

[48] J. Enders, N. Huxel, P. von Neumann-Cosel, and A. Richter, Phys. Rev. Lett. **79**, 2010 (1997).

[49] N. Lo Iudice, E. Lipparini, S. Stringari, F. Palumbo, and A. Richter, Phys. Lett. B **161**, 18 (1985).

[50] C. P. Brits, K. L. Malatji, M. Wiedeking, B. V. Kheswa, S. Goriely, F. L. Bello Garrote, D. L. Bleuel, F. Giacoppo, A.

Gorgen, M. Guttormsen, K. Hadynska-Klek, T. W. Hagen, S. Hilaire, V. W. Ingeberg, H. Jia, M. Klintefjord, A. C. Larsen, S. N. T. Majola, P. Papka, S. Peru, B. Qi, T. Renstrøm *et al.*, Phys. Rev. C **99**, 054330 (2019).

[51] M. Guttormsen, L. A. Bernstein, A. Bürger, A. Görgen, F. Gunsing, T. W. Hagen, A. C. Larsen, T. Renstrøm, S. Siem, M. Wiedeking, and J. N. Wilson, Phys. Rev. Lett. **109**, 162503 (2012).